



# Microbial CO<sub>2</sub> assimilation is not limited by the decrease in autotrophic bacterial abundance and diversity in eroded watershed

Haibing Xiao<sup>1,2</sup> · Zhongwu Li<sup>1,3</sup> · Xiaofeng Chang<sup>1</sup> · Lei Deng<sup>1</sup> · Xiaodong Nie<sup>4</sup> · Chun Liu<sup>3</sup> · Lin Liu<sup>1</sup> · Jieyu Jiang<sup>3</sup> · Jia Chen<sup>1,2</sup> · Danyang Wang<sup>3</sup>

Received: 13 January 2018 / Revised: 25 April 2018 / Accepted: 27 April 2018 / Published online: 5 May 2018  
© Springer-Verlag GmbH Germany, part of Springer Nature 2018

## Abstract

The impacts of soil erosion on soil structure, nutrient, and microflora have been extensively studied but little is known about the responses of autotrophic bacterial community and associated carbon (C)-fixing potential to soil erosion. In this study, three abandoned croplands (ES1, ES2, and ES3) and three check dams (DS1, DS2, and DS3) in the Qiaozi watershed of Chinese Loess Plateau were selected as eroding sites and depositional sites, respectively, to evaluate the impacts of soil erosion on autotrophic bacterial community and associated C-fixing potential. Lower abundance and diversity of autotrophic bacteria were observed in nutrient-poor depositional sites compared with nutrient-rich eroding sites. However, the relative abundances of obligate autotrophic bacteria, such as *Thiobacillus* and *Synechococcus*, were significantly enhanced in depositional sites. Deposition of nutrient-poor soil contributed to the growth of obligate autotrophic bacteria. The maximum microbial C-fixing rate was observed in DS1 site ( $5.568 \pm 1.503 \text{ Mg C km}^{-2} \text{ year}^{-1}$ ), followed by DS3 site ( $5.306 \pm 2.130 \text{ Mg C km}^{-2} \text{ year}^{-1}$ ), and the minimum was observed in ES2 site ( $0.839 \pm 0.558 \text{ Mg C km}^{-2} \text{ year}^{-1}$ ). Soil deposition significantly enhanced microbial C-fixing rate. Assuming a total erosion area of  $1.09 \times 10^7 \text{ km}^2$ , microbial C-fixing potential in eroded landscape can range from 0.01 to 0.06 Pg C year<sup>-1</sup>. But its effect on the C pool recovery of degraded soil is limited. Dissolved organic C (DOC) was the main explanatory factor for the variation in soil microbial C-fixing rate (72.0%,  $P = 0.000$ ).

**Keywords** Soil erosion · Organic carbon · Autotrophic bacteria · Carbon-fixing potential · Chinese Loess Plateau

**Electronic supplementary material** The online version of this article (<https://doi.org/10.1007/s00374-018-1284-7>) contains supplementary material, which is available to authorized users.

✉ Zhongwu Li  
lizw@hnu.edu.cn

<sup>1</sup> State Key Laboratory of Soil Erosion and Dryland Farming on the Loess Plateau, Institute of Soil and Water Conservation CAS and MWR, Yangling 712100, Shaanxi, People's Republic of China

<sup>2</sup> University of Chinese Academy of Sciences, Beijing 100000, People's Republic of China

<sup>3</sup> College of Environmental Science and Engineering, Hunan University, Changsha 410082, People's Republic of China

<sup>4</sup> Guangdong Key Laboratory of Integrated Agro-environmental Pollution Control and Management, Guangdong Institute of Eco-environmental Science & Technology, Guangzhou 510650, People's Republic of China

## Introduction

Soil erosion is one of the major soil degradation processes. On Chinese Loess Plateau, the high-intensity storms and friable soil can accelerate this degradation resulting in the mean soil loss rate of 50–100 Mg ha<sup>-1</sup> year<sup>-1</sup> (Li et al. 2017). Various engineering and biological measures, such as check dam construction and vegetation restoration, had been used to restore the degraded soil and control soil loss (Xu et al. 2004). By 2002, approximately 113,500 check dams had been constructed in the Loess Plateau and more than 700 million m<sup>3</sup> sediments had been intercepted by them (Wang et al. 2017; Xu et al. 2004). Erosion process not only has important impacts on soil loss but also significantly affects the distribution, mineralization, and sequestration of soil organic C (SOC) (Afshar et al. 2010; Berhe et al. 2007; Doetterl et al. 2012; Nie et al. 2018; Polyakov and Lal 2004), but there have been contrasting results over the relationship between soil erosion and C dynamic. On one hand, Stallard (1998) suggested that the sedimentation of eroded soil can contribute to soil C

sequestration with a capacity of 0.6 to 1.5 Pg C year<sup>-1</sup> according to hydrologic-biogeochemical models. On the contrary, Jacinthe and Lal (2001) and Lal (2003, 2005) indicated that soil erosion constitutes a source of atmospheric CO<sub>2</sub> with a capacity of 0.37 to 1.0 Pg C year<sup>-1</sup>. Polyakov and Lal (2008) showed that significant amounts of SOC mobilized by erosion (15%) could be released to the atmosphere within 100 days incubation of eroded sediments due to the breakdown of initial soil aggregates. Xiao et al. (2017a) investigated the relationships between SOC mineralization and abiotic and biotic soil properties in eroded agricultural lands and suggested that the effects of changing microbial abundance and species diversity on SOC mineralization were smaller than the potential effects of organic matter quality changes. Despite changes in soil C pools caused by erosion and its influencing mechanisms were widely explored over past decades, the responses of autotrophic bacterial community and associated C-fixing potential to soil erosion are poorly known.

Many microbial species in soil, such as *Azospirillum lipoferum*, *Bradyrhizobium japonicum*, *Ralstonia eutropha*, and *Prochlorococcus*, can fix atmospheric CO<sub>2</sub> (Yuan et al. 2012c). The Calvin-Benson-Bassham (CBB) cycle is the predominant pathway for autotrophic bacteria to assimilate atmospheric CO<sub>2</sub> and the ribulose-1,5-bisphosphate carboxylase oxygenase (RubisCO) is the rate-limiting enzyme in this cycle (Long et al. 2015). Thus, the *cbbl* gene encoding the large subunit of RubisCO (form I) has been widely used as a functional marker to analyze the autotrophic bacterial community (Selesi et al. 2007). Autotrophic bacteria can play an important role in soil C fixation (Ge et al. 2012; Wu et al. 2015; Yuan et al. 2012a, c). By investigating microbial CO<sub>2</sub> assimilation in paddy ecosystems, Ge et al. (2012) showed that after continuous labeling for 80 days with <sup>14</sup>C-CO<sub>2</sub>, the <sup>14</sup>C-SOC fixed by autotrophic bacteria ranged from 114.3 to 348.2 mg kg<sup>-1</sup>, accounting for 0.73 to 1.99% of total SOC. Yuan et al. (2012a) showed that microbial assimilation of <sup>14</sup>C-CO<sub>2</sub> accounted for 0.12 to 0.59% of SOC in paddy and upland soils. Assuming a terrestrial area of 1.4 × 10<sup>8</sup> km<sup>2</sup>, the potential global sequestration is 0.6–4.9 Pg C year<sup>-1</sup>. Therefore, understanding the influencing mechanisms of soil erosion on autotrophic bacterial community and associated C-fixing rate is very important for determining the role of soil erosion on global C cycle. The objectives of this study are to (i) investigate the response patterns of autotrophic bacterial communities to soil erosion, (ii) explore the differences in microbial C-fixing rate between eroding and depositional sites, and (iii) analyze the relationships between microbial C-fixing rate and soil biotic and abiotic properties. Soil deposition always increases soil organic matter content (Li et al. 2015) and the increase in soil nutrient content contributes to increase autotrophic bacterial abundance and diversity (Ge et al. 2016; Yuan et al. 2012b, c). Thus, in this study, we hypothesized that (H1) the abundance and diversity of autotrophic bacteria in depositional sites were

significantly higher than eroding sites, and that (H2) microbial C-fixing rate was mainly controlled by autotrophic bacterial biomass. To test our hypotheses, abandoned croplands and check dams were selected as eroding and depositional sites in the Qiaozhi watershed of Chinese Loess Plateau, respectively. High-throughput sequencing of *cbbl* gene was applied to determine the composition of autotrophic bacteria and <sup>13</sup>C stable isotope tracer technique was used to estimate microbial C-fixing rate.

## Materials and methods

### Study area

This study was conducted in the Qiaozhi watershed (34° 36'–34° 37' N, 105° 42'–105° 43' E), which is situated near the city of Tianshui, Gansu province, on the Chinese Loess Plateau. The elevation of the watershed ranges from 1330 to 1707 m. The climate in this region is semi-arid and continental, with a mean annual temperature of 10.7 °C and an average annual precipitation of 496–628 mm. More than 60% of the precipitation falls in the rainy season (June to September) mainly as high-intensity rainstorms (Zhou et al. 2012). The main soil type is black cinnamonic soil (Calcic Cambisol, FAO), which is silty in texture (9% sand, 71% silt, and 20% clay) and weakly resistant to erosion. Soil erosion in this watershed mainly consists of water erosion and gravity erosion, with the annual sediment yield of 2026 Mg km<sup>-2</sup> (Liu et al. 2017).

To control the erosion, various engineering and biological measures, such as check dam construction, terracing, and vegetation restoration, had been conducted by the local government. Since the 1990s, 22 check dams had been constructed in this area (Li et al. 2017). In the upper part of the watershed, cropland and abandoned cropland are the primary sediment sources. The main crop grown on the land was maize (*Zea mays* L.), and the dominant plants after 11 years of abandonment were *Heteropappus altaicus* and *Artemisia capillaries* (Table S1). To explore the differences in autotrophic bacterial community and associated C-fixing rate between eroding and depositional sites, three abandoned croplands and three check dams (the main parameters are shown in Table S2) were selected and represented the eroding and depositional sites in the watershed, respectively. The vegetation type of check dams was similar with the abandoned croplands. The main characteristics of the study sites are shown in the Table S1.

### Soil sampling and treatment

A 20 m × 40 m and 10 m × 20 m sampling plot was selected at each eroding (abandoned cropland) and depositional

(check dam) site, respectively. Six quadrats (2 m × 2 m) were randomly placed in each sampling plot of the eroding site, and three quadrats (2 m × 2 m) were randomly selected in each sampling plot of the depositional site. In August 2016, nine 0–10-cm soil samples were collected in each quadrat with a 5-cm diameter corer and then mixed together. Additionally, to evaluate the erosion and deposition status, a composite sample consisted of nine 0–30-cm soil samples was collected in each quadrat for the analysis of  $^{137}\text{Cs}$  activity. A total of 27 composite soil samples (3 eroding sites × 6 quadrats + 3 depositional sites × 3 quadrats) and 27  $^{137}\text{Cs}$  composite samples were collected in the study sites. All collected samples were instantly transported into the laboratory. Each soil sample was divided into two parts: one was sieved (< 2 mm) and immediately stored at  $-70\text{ }^\circ\text{C}$  for later isotope labeling experiment; the other part was air-dried prior to the determination of physicochemical soil properties. The  $^{137}\text{Cs}$  samples were air-dried for the estimation of  $^{137}\text{Cs}$  inventory ( $\text{Bq m}^{-2}$ ).

### Incubation experiment with $^{13}\text{C}$ -labeled $\text{CO}_2$

To stabilize the microbial activity, 50 g (dry weight) sieved fresh soil (< 2 mm) was adjusted to 60% water holding capacity and then pre-incubated in a 500-ml Erlenmeyer flask (soil depth approximately 5 cm) under light (500 mmol photons  $\text{m}^{-2} \text{s}^{-1}$ ) conditions at  $25\text{ }^\circ\text{C}$  for 15 days (Ge et al. 2013). After pre-incubation, artificial air (79%  $\text{N}_2$  and 21%  $\text{O}_2$ ) was flushed into the flask to remove the atmospheric  $\text{CO}_2$ , and then the flask was instantly sealed with a rubber stopper. Two sets of microcosms were established in our experiment. The first set 0.2 ml  $^{13}\text{C}$ - $\text{CO}_2$  (99 atom %, Newradar Special Gas  $\text{CO}_2$ , Wuhan, China) was injected into the flask; in the other set, the control, 0.2 ml  $^{12}\text{C}$ - $\text{CO}_2$  was added. The  $\text{CO}_2$  level of both sets of microcosms was maintained at approximately 400 ppm. Three replicates were established for each soil sample, thus giving 162 microcosms (2 sets × 27 soil samples × 3 replicates) that were prepared.

All microcosms were incubated in a chamber for 80 days. During the incubation period, all microcosms were illuminated with an intensity of 500 mmol photons  $\text{m}^{-2} \text{s}^{-1}$  for 12 h each day (8:00 am to 8:00 pm). Day/night temperatures inside the chamber were set at  $25 \pm 1/15 \pm 1\text{ }^\circ\text{C}$ , respectively, and the relative humidity was maintained at 80% (Wu et al. 2014). In order to maintain aerobic condition and a constant  $\text{CO}_2$  level, the microcosms were periodically (every 5 days) aerated with artificial air and injected with  $^{13}\text{C}$ - $\text{CO}_2$ / $^{12}\text{C}$ - $\text{CO}_2$  (0.2 ml). At the end of incubation, each microcosm was mixed thoroughly and then divided into two portions: one was air-dried at room temperature to determine the concentration of  $^{13}\text{C}$ -SOC;

the other portion was stored at  $-70\text{ }^\circ\text{C}$  for molecular analysis.

## Laboratory analyses

### Measurement of physicochemical soil properties

The sieved (< 2 mm) and air-dried soil samples were analyzed for soil pH and particle size distribution. Soil pH was determined with a soil-to-water ratio of 1:2.5 ( $w/v$ ) using a digital pH meter (Woonsocket, RI, USA). The particle size distribution was analyzed with a laser particle size analyzer (MS-2000, Malvern, UK). Soil bulk density (BD) was measured by the cutting ring method. Subsamples passed through a 1-mm mesh sieve were analyzed for available nitrogen (N) using the alkali N proliferation method (Cornfield 1960). Subsamples passed through a 0.149-mm mesh sieve were analyzed for their SOC and total N (TN) contents. The SOC content was measured using the dichromate oxidation method (Walkley and Black 1934) and TN by the Kjeldahl (1883) method. Dissolved organic C (DOC) and microbial biomass C (MBC) were measured according to Xiao et al. (2017b). The main physicochemical soil properties are presented in the Table 1.

Air-dried  $^{137}\text{Cs}$  samples (0–30 cm) were sieved (< 2 mm) and the fine fraction was analyzed for  $^{137}\text{Cs}$  activity. The  $^{137}\text{Cs}$  activity was determined via gamma spectrometry using a hyper-pure germanium detector coupled to a multi-channel digital analyzer system (ORTEC, Oak Ridge, TN, USA) with average counting time over 40,000 s. The gamma emission of  $^{137}\text{Cs}$  was determined at 661.6 keV (Wang et al. 2017).

### Measurement of $^{13}\text{C}$ -SOC concentration

According to Ge et al. (2016), 3.0 ml 2.5 M HCl was added and mixed with 1.50 g air-dried soil (passed through 0.149-mm sieve) in Dolphin tubes for 24 h to remove inorganic C from soil. Then, the soil was washed with 3.0 ml ultrapure water twice to clean the remaining HCl. The stable C isotope ratio of HCl-treated soil samples was measured using a MAT253 isotope ratio mass spectrometer coupled to an elemental FLASH HT (ThermoFisher Scientific, Waltham, MA, USA). The amount of  $^{13}\text{C}$ -SOC ( $\text{mg kg}^{-1}$ ) was calculated according to Yuan et al. (2016). The synthesis rate of  $^{13}\text{C}$ -SOC ( $\text{Mg km}^{-2} \text{ year}^{-1}$ ) was calculated as follows:

$$RS = {}^{13}\text{C-SOC} \times BD \times D \times R/1000 \quad (1)$$

where  $RS$  is the synthesis rate of  $^{13}\text{C}$ -SOC ( $\text{Mg km}^{-2} \text{ year}^{-1}$ ),  ${}^{13}\text{C-SOC}$  is the content of SOC labeled by  $^{13}\text{C}$  ( $\text{mg kg}^{-1}$ ),  $BD$

**Table 1** Soil physicochemical properties in eroding and depositional sites

Sites	Moisture (%)	BD (g cm <sup>-3</sup> )	pH	Sand (%)	Silt (%)	Clay (%)
ES1 <sup>a</sup>	10.87 (0.91)	1.32 (0.13)	8.33 (0.02)	15.09 (2.45)	63.49 (1.45)	21.42 (1.67)
ES2	11.02 (0.89)	1.29 (0.19)	8.32 (0.06)	14.69 (2.34)	65.01 (1.55)	20.30 (2.66)
ES3	12.20 (3.07)	1.28 (0.13)	8.40 (0.10)	14.93 (3.08)	64.87 (2.30)	20.20 (2.42)
ES group	11.37 (0.73) a <sup>b</sup>	1.30 (0.02) a	8.35 (0.04) b	14.90 (0.20) a	64.46 (0.84) b	20.64 (0.68) a
DS1	12.04 (3.31)	1.26 (0.15)	8.60 (0.04)	12.18 (0.75)	68.54 (0.68)	19.28 (0.59)
DS2	8.52 (1.21)	1.49 (0.24)	8.45 (0.17)	8.83 (6.75)	70.26 (4.02)	20.91 (3.22)
DS3	11.82 (1.37)	1.47 (0.21)	8.65 (0.08)	8.92 (5.07)	69.19 (2.97)	21.89 (3.05)
DS group	11.83 (1.97) a	1.41 (0.13) a	8.57 (0.10) a	9.98 (1.91) b	69.33 (0.87) a	20.69 (1.32) a

BD bulk density

<sup>a</sup> ES1, ES2, and ES3 are the three replicates of the eroding site (ES group: abandoned cropland); DS1, DS2, and DS3 are the three replicates of the depositional site (DS group: check dam)

<sup>b</sup> Numbers in brackets are the standard errors of means, and different letters in the same column indicate significant differences at the  $P < 0.05$  level based on least significant difference analysis

is the bulk soil density (kg m<sup>-3</sup>),  $D$  is the sampling depth (m), and  $R$  is the time ratio (365/80).

### Determination of the composition of autotrophic bacteria

Genomic DNA was extracted using a PowerSoil DNA isolation kit (MoBio Laboratories, Carlsbad, USA) from the soil samples following the manual. The quantity and quality of the DNA extracts were evaluated by agarose gel (1%) electrophoresis and an ultraviolet spectrophotometer (Nanodrop 2000, Thermo Scientific, Wilmington, USA). The primers K2f (5'-ACCAAYCAAGCCSAAGCTSGG-3') and V2r (5'-GCCTTCSAGCTTGCCSACCRC-3') were used to amplify the target *cbbL* gene fragment (Keshri et al. 2015). For each soil sample, a 10-digit barcode sequence was added to the 5' end of the forward and reverse primers. The PCR reaction was performed on a GeneAmp PCR System 9700 (Applied Biosystem, Waltham, USA) with a 25 µl reaction mixture, containing 30 ng template DNA, 3 µl BSA (2 ng µl<sup>-1</sup>), 12.5 µl 2× Taq PCR MasterMix, and 1 µl barcoded primers K2f and V2r each. The PCR conditions were as follows: an initial denaturation step performed at 95 °C for 5 min followed by 30 denaturation (95 °C, 60 s), annealing (52 °C, 60 s) and extension (72 °C, 60 s) cycles, and a final extension at 72 °C for 10 min (Esparza et al. 2010). The purified PCR amplicons were pooled to reach equimolar ratios and paired-end sequenced (2 × 250) on the Illumina Miseq PE300 platform (Illumina, USA) at the Beijing Allwegene Technology Co., Ltd. Clustering of the screened *cbbL* gene sequences (whose number ranged from 32,394 to 77,823) into operational taxonomic units (OTUs) was performed using UPARSE (Uparse v.7.0.1001) at a 97% sequence similarity. Good's coverage, Shannon index, and rarefaction curve were calculated by the MOTHUR software package (version 1.30.0). The rarefaction

curves reached asymptotes for all samples (Fig. S1), which indicated that the sequencing depth was high enough to cover the microbial diversity (Schöler et al. 2017; Vestergaard et al. 2017).

### Quantification of autotrophic bacterial abundance

The real-time qPCR was conducted on an ABI7500 PCR system (Applied Biosystems, USA) using a total volume of 50 µl containing 1 µl purified DNA template, 1 µl each prime (10 µM), 25 µl PremiSTAR HS Premix (Takara), and 22 µl sterile water. The PCR conditions were pre-denaturation at 94 °C for 5 min followed by 30 cycles consisting of 94 °C for 30 s, 55 °C for 30 s, and 72 °C for 30 s (Videmsek et al. 2009). Amplification of each sample was replicated three times and the mean value was used for the subsequent analysis. The standard curve for qPCR was created using 10-fold dilution series (ranging from  $1.0 \times 10^3$  to  $1.0 \times 10^9$ ) of plasmid DNA. To determine the specificity of PCR products, melt curve analysis was performed at the end of PCR cycle and a single melt curve peak was observed for each sample.

### Statistical analyses

All variables were tested for normality using a Kolmogorov-Smirnov test. Autotrophic bacterial abundance was log<sub>10</sub>-transformed to meet the normality assumption of ANOVA. One-way analysis of variance (ANOVA), followed by a least square difference (LSD) post hoc test ( $P < 0.05$ ), was performed to determine the significant difference among the means. Pearson's correlation analysis was used for assessing the association between variables. In addition, multiple stepwise regression was used to analyze the contributions of abiotic and biotic soil properties to the variation in microbial C-fixing rate. In total, nine abiotic soil properties (SOC, TN,

available N, DOC, MBC, pH, sand, silt, and clay) and two biotic properties (autotrophic bacterial abundance and Shannon index) were selected. All explanatory variables (abiotic and biotic parameters) were checked for collinearity, and the variance inflation factors (VIFs) were  $< 2$ . All statistical analyses were performed using the software program SPSS ver. 19.0 (SPSS Inc., Chicago, IL, USA).

### Nucleotide sequence accession numbers

The nucleotide sequences of *cbbL* determined in the study have been deposited in the GenBank database under accession numbers of SRR6175410 to SRR6175427.

## Results

### Negative responses of $^{137}\text{Cs}$ inventory and nutrients to soil deposition

The  $^{137}\text{Cs}$  inventory ranged from 116.93 to 1322.86  $\text{Bq m}^{-2}$  and ranked as follows: ES3 > ES1 > ES2 > DS2 > DS1 > DS3. Statistical analysis showed that the average  $^{137}\text{Cs}$  values in the ES sites were significantly ( $P < 0.05$ ) higher than that in the DS sites, but all values were below the  $^{137}\text{Cs}$  reference value ( $1400.68 \pm 449.50 \text{ Bq m}^{-2}$ ) (Fig. 1). The SOC and TN content ranged from 3.69 to 11.10 and 0.62 to 1.68  $\text{mg g}^{-1}$ , respectively. The average SOC content in the ES group ( $8.26 \text{ mg g}^{-1}$ ) was greater ( $P < 0.05$ ) than that in the DS group ( $6.52 \text{ mg g}^{-1}$ ) (Fig. 2a), while the average TN content was

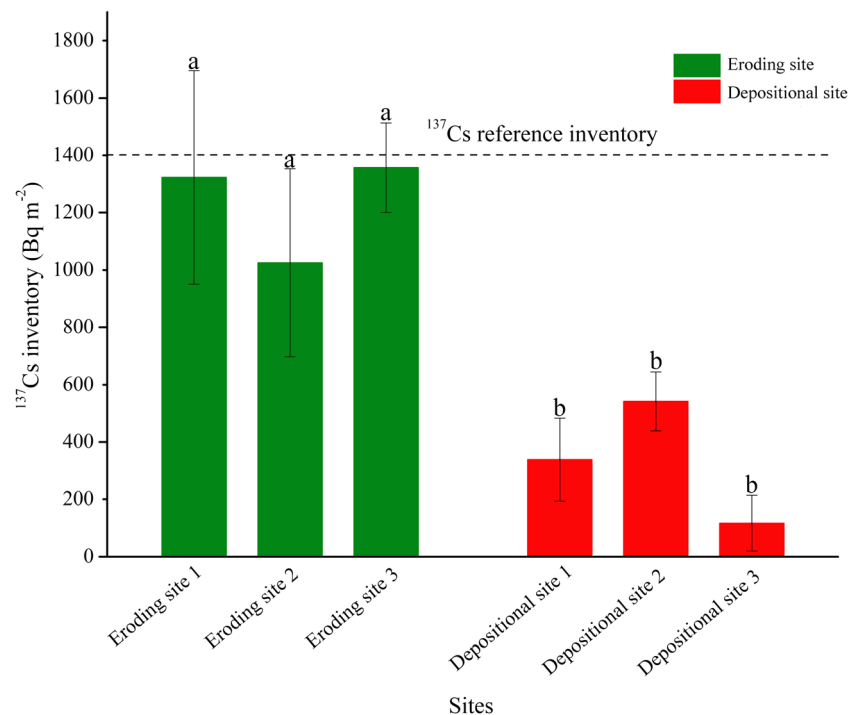
similar ( $P > 0.05$ ) between the two groups (Fig. 2b). The average DOC and MBC contents were higher ( $P < 0.05$ ) in the ES group ( $0.16$  and  $1.27 \text{ mg g}^{-1}$ , respectively) than those in the DS group ( $0.08$  and  $1.04 \text{ mg g}^{-1}$ , respectively) (Fig. 2d, e). The average available N concentration of the ES group was similar with that of the DS group ( $P > 0.05$ ) (Fig. 2c). The average C/N in the ES group was 1.26 times higher than that in the DS group (Fig. 2f).

### Autotrophic bacterial abundance positively correlated with soil nutrients

The autotrophic bacterial abundance ranged from  $2.58 \times 10^7$  to  $8.61 \times 10^7$  copies  $\text{g}^{-1}$  soil and ranked as follows: ES3 > ES2 > ES1 > DS2 > DS3 > DS1. Statistical analysis showed that the average autotrophic bacterial abundance in the ES group ( $7.19 \times 10^7$  copies  $\text{g}^{-1}$  soil) was significantly ( $P < 0.05$ ) higher than that in the DS group ( $4.23 \times 10^7$  copies  $\text{g}^{-1}$  soil) (Table 2). The coverage indices for all sites were greater than 0.99, which indicated that our data captured most of autotrophic bacterial species. Compared with the DS group, the Shannon index in the ES group was significantly ( $P < 0.05$ ) increased (Table 2).

Average *Proteobacteria* abundance, accounted for 91.1 to 96.7% of the OTUs of the two groups, was the dominant autotrophic bacterial phylum (Fig. 3a). Average *Beta-proteobacteria* abundance represented 67.9 and 60.1% of the OTUs in the ES and DS groups, respectively (Fig. 3b), and it was the main autotrophic bacterial class. At the order level, *Burkholderiales* (52.5%) and *Hydrogenophilaales* (31.7%)

**Fig. 1** The  $^{137}\text{Cs}$  inventory of eroding (green color) and depositional sites (red color). The error bars represent the standard errors of means. Plots labeled with the same letter are not significantly different at  $P < 0.05$  level



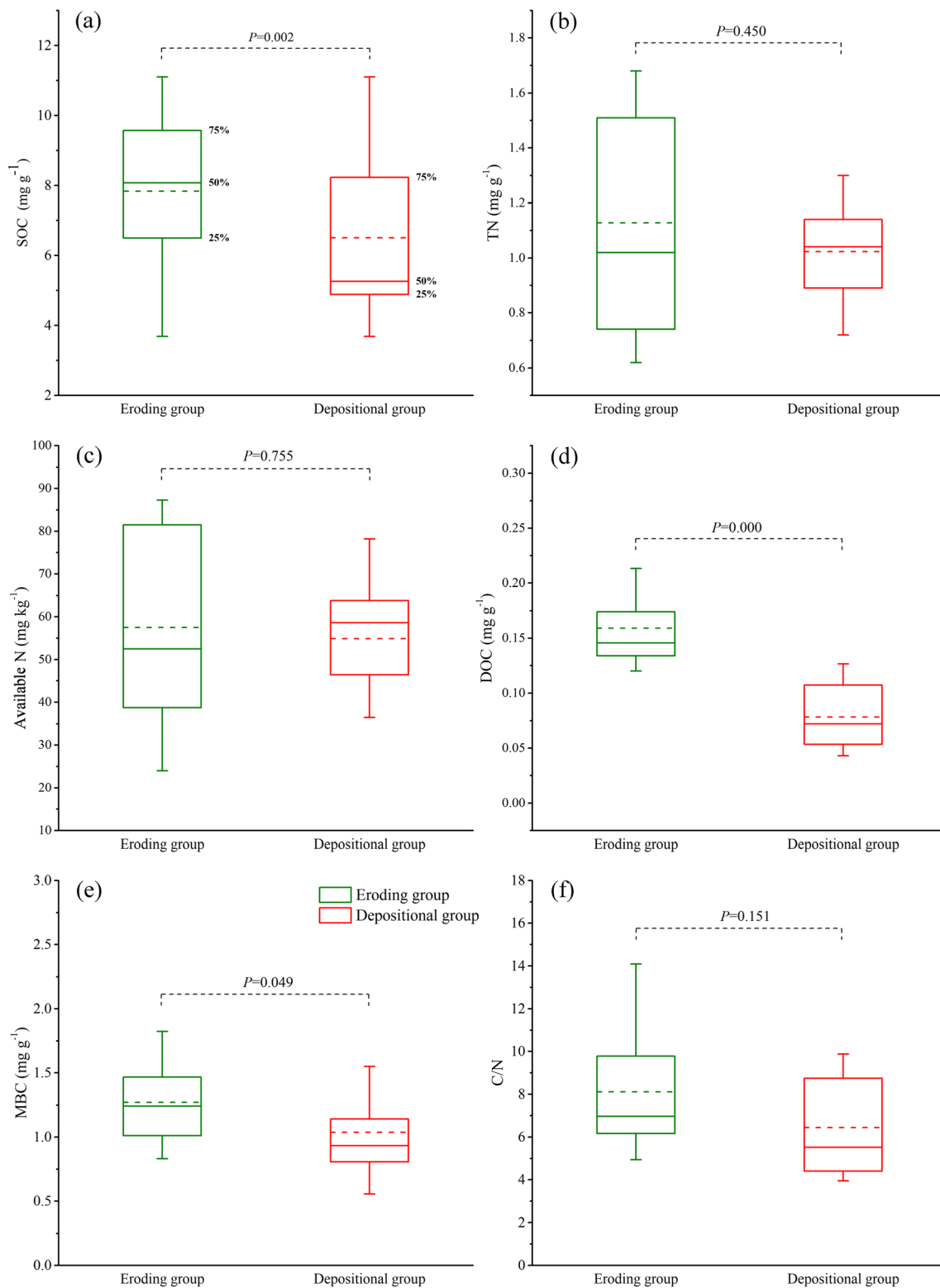


**Fig. 2** The content of **a** soil organic C (SOC), **b** total N (TN), **c** available N (AN), **d** dissolved organic C (DOC), **e** microbial biomass C (MBC), and **f** the C/N ratio of eroding (green color) and depositional (red color)

groups.  $P < 0.05$  indicates statistically significant difference between eroding and depositional groups. The dash line in the box represents the mean value

were the dominant bacterial taxa in the ES and DS groups, respectively. Compared with the ES group, the relative average abundances of *Hydrogenophilales*, *Rhodobacterales*, and

*Synechococcales* were significantly improved ( $P < 0.05$ ) in the DS group, while the relative average abundances of *Burkholderiales* and *Nitrosomonadales* were ( $P < 0.05$ )

**Table 2** The abundance and Shannon index of autotrophic bacteria in the study sites

Sites	Coverage index	OTUs	Abundance (copies g <sup>-1</sup> soil)	Shannon index
ES1 <sup>a</sup>	0.997	351 (9)	6.44 × 10 <sup>7</sup> (2.08 × 10 <sup>7</sup> )	5.77 (0.11)
ES2	0.997	364 (24)	6.52 × 10 <sup>7</sup> (1.42 × 10 <sup>7</sup> )	5.67 (0.21)
ES3	0.997	362 (7)	8.61 × 10 <sup>7</sup> (5.11 × 10 <sup>7</sup> )	5.41 (0.04)
ES group	0.997 a <sup>b</sup>	359 (14) b	7.19 × 10 <sup>7</sup> (3.04 × 10 <sup>7</sup> ) a	5.62 (0.20) a
DS1	0.997	356 (16)	2.58 × 10 <sup>7</sup> (2.26 × 10 <sup>7</sup> )	4.77 (0.50)
DS2	0.997	412 (17)	6.39 × 10 <sup>7</sup> (2.16 × 10 <sup>7</sup> )	4.88 (0.49)
DS3	0.997	393 (20)	3.73 × 10 <sup>7</sup> (1.05 × 10 <sup>7</sup> )	5.81 (0.20)
DS group	0.997 a	387 (29) a	4.23 × 10 <sup>7</sup> (2.36 × 10 <sup>7</sup> ) b	5.15 (0.61) b

OTUs operational taxonomic units

<sup>a</sup> ES1, ES2, and ES3 are the three replicates of the eroding site (ES group: abandoned cropland); DS1, DS2, and DS3 are the three replicates of the depositional site (DS group: check dam)

<sup>b</sup> Numbers in brackets are the standard errors of means, and different letters in the same column indicate significant differences at the *P* < 0.05 level based on least significant difference analysis

decreased (Fig. 4a). At the genus level, *Thiobacillus* was the main bacterial genus in ES (12.1%) and DS (31.7%) groups. Statistical analysis showed that the relative average abundances of *Thiobacillus*, *Rhodobacter*, and *Synechococcus* in the DS group were significantly (*P* < 0.05) higher than those in the ES group (Fig. 4b). Correlation analysis showed that SOC, DOC, and MBC were positively correlated with total autotrophic bacterial abundance (Table S3), while negatively correlated with the relative abundances of *Thioalkalivibrio*, *Rhodobacter*, and *Synechococcus* (Fig. 5).

### Deposition of nutrient-poor soil increased microbial C-fixing rate

After 80 days of incubation, the amount of SOC labeled by <sup>13</sup>C was determined. The average amount of <sup>13</sup>C-SOC ranged from 1.36 (ES2) to 9.06 (DS1) mg kg<sup>-1</sup> and differed significantly (*P* < 0.05) between eroding and depositional sites. The average <sup>13</sup>C-SOC amount in the DS group was 4.53 times

higher than that in the ES group (Table 3). The percentage of SOC present as <sup>13</sup>C-SOC (<sup>13</sup>C-SOC/SOC, %) ranged from 0.019% (ES2) to 0.172% (DS1) and was significantly (*P* < 0.05) lower in the ES group (0.023%) than that in the DS group (0.119%) (Table 3). The synthesis rate of <sup>13</sup>C-SOC ranked as follows: DS1 > DS3 > DS2 > ES3 > ES1 > ES2, and the average value of the DS group was 4.67 times higher than that in the ES group (Table 3).

Correlation analysis showed that <sup>13</sup>C-SOC content and its synthesis rate were negatively correlated (*P* < 0.05) with SOC and DOC contents and the abundance and Shannon index of autotrophic bacteria (Table S3), while positively correlated (*P* < 0.05) with the relative abundances of *Thiobacillus*, *Rhodobacter*, and *Synechococcus* (Fig. 5). In addition, multiple linear regression analysis indicated that the synthesis rate of <sup>13</sup>C-SOC was primarily influenced (*P* < 0.05) by DOC and sand contents and autotrophic bacterial diversity. DOC, which explained up to 72% of the variation, was the main influencing factor for microbial C-fixing rate. Sand content and

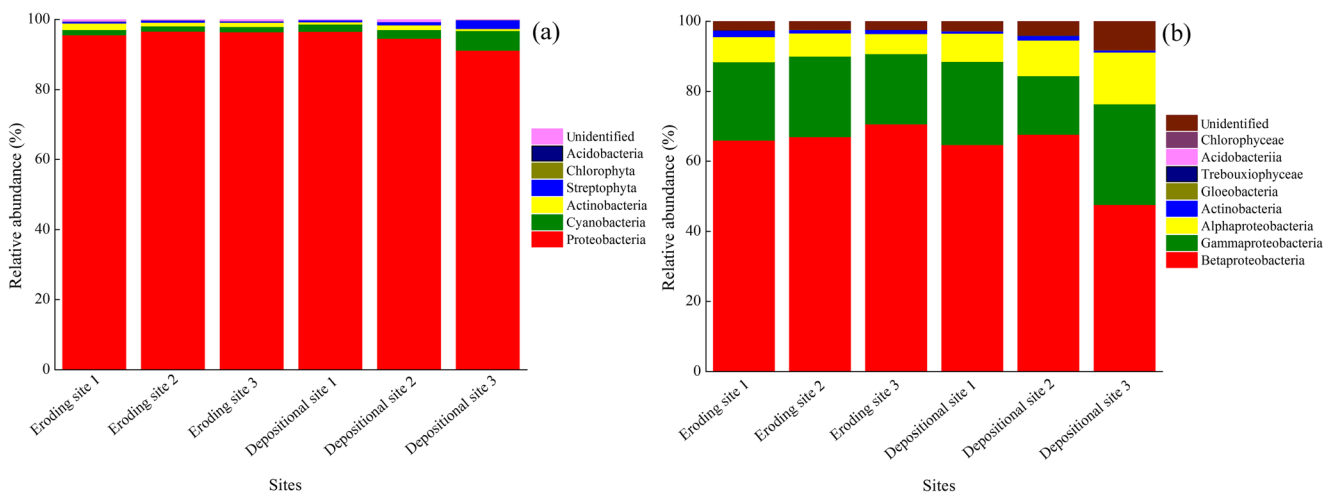


**Fig. 3** Phylum (a) and class (b) of autotrophic bacterial community across different sites

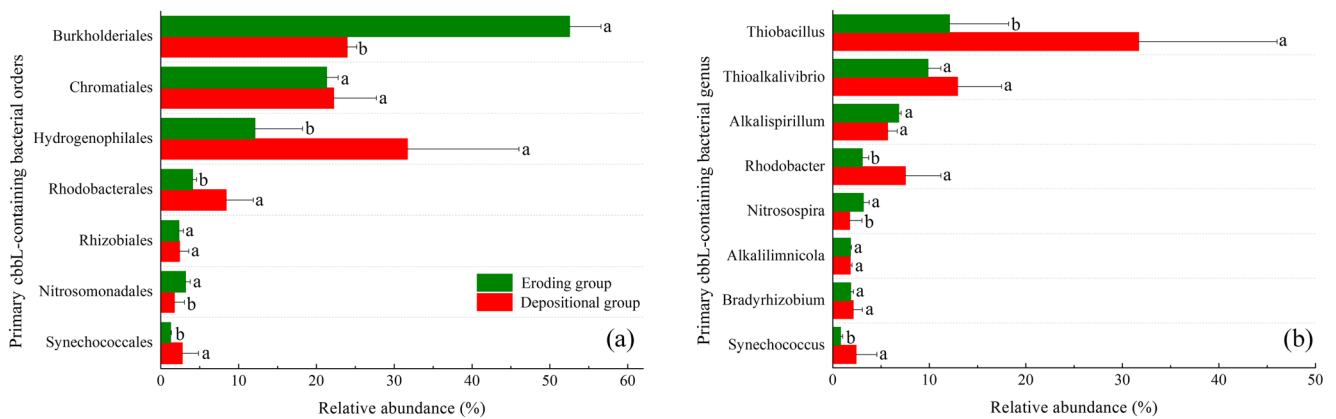


**Fig. 4** The relative abundances of major bacterial taxa (*cbbL*-containing) at order (a) and genus (b) levels between eroding (green color) and depositional (red color) groups

Shannon index explained 12.8 and 4.3% of the variation, respectively (Table 4).

## Discussion

Radionuclide  $^{137}\text{Cs}$  was applied to confirm the erosion or deposition status in the studied sites. Once the  $^{137}\text{Cs}$  fallout reaches the earth's surface, it is strongly and rapidly adsorbed by fine soil colloidal particles, such as clay minerals and organic matter, in the topsoil. Chemical or biological removal of  $^{137}\text{Cs}$  from soil particles is limited and it is assumed that only physical processes moving soil particles such as soil erosion are involved in the  $^{137}\text{Cs}$  transport (Afshar et al. 2010; Gaspar and Navas 2013). Therefore, compared with the  $^{137}\text{Cs}$  reference value, lower  $^{137}\text{Cs}$  inventory in eroding sites and higher

$^{137}\text{Cs}$  inventory in depositional sites would be observed in eroded hillslopes and watersheds due to the transportation of  $^{137}\text{Cs}$ -rich topsoil from eroding sites to depositional sites during interrill erosion (Li et al. 2015; Xiao et al. 2017a). As we expected, the  $^{137}\text{Cs}$  inventories in abandoned croplands were below the reference value, which indicated abandoned cropland was the important sediment source of Qiaozi watershed. However, the  $^{137}\text{Cs}$  inventories in the check dams, as sediment deposition sites, were significantly lower than the reference value even the values in eroding sites (abandoned croplands), which was opposite to our hypothesis. This inconsistent result might be related to the accumulation of  $^{137}\text{Cs}$ -depleted soil in check dams. To prevent soil loss, check dams were constructed in erosion gullies, which collected the runoff and sediments coming from the upper watershed. The runoff transported the  $^{137}\text{Cs}$ -depleted soil at the bottom of

**Fig. 5** Correlation analysis between selected bacterial genera and abiotic soil properties (\* $P < 0.05$ ; \*\* $P < 0.01$ ). SOC soil organic C, TN total N, DOC dissolved organic C, MBC microbial biomass C, BD bulk density,  $^{13}\text{C}$ -SOC soil organic C labeled by  $^{13}\text{C}$ , RS synthesis rate of  $^{13}\text{C}$ -SOC

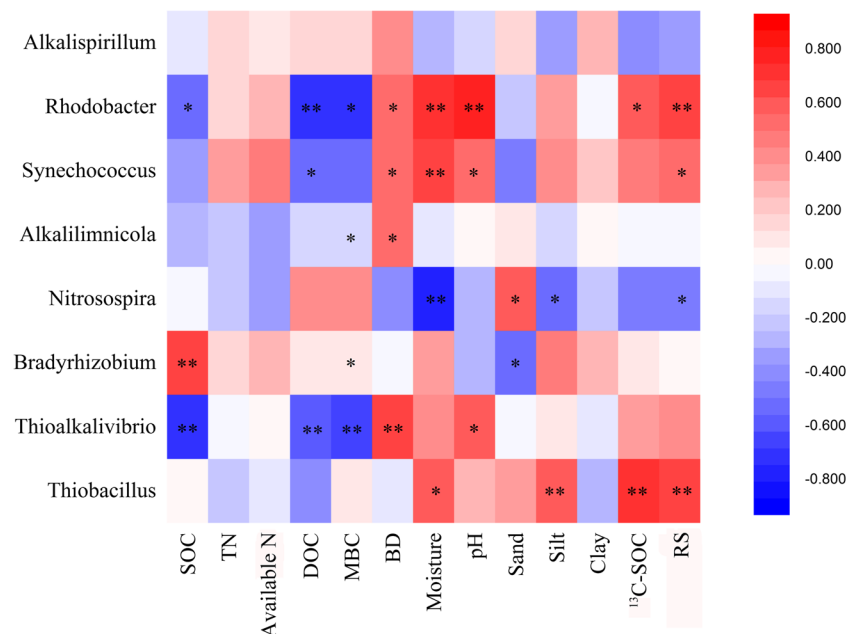




**Table 3** <sup>13</sup>C-SOC, percentage of SOC present as <sup>13</sup>C-SOC to SOC, and synthesis rate of <sup>13</sup>C-SOC in the study sites

Sites	<sup>13</sup> C-SOC (mg kg <sup>-1</sup> )	<sup>13</sup> C-SOC/SOC (%)	RS (Mg C km <sup>-2</sup> year <sup>-1</sup> )
ES1 <sup>a</sup>	1.78 (1.02)	0.023 (0.014)	1.088 (0.636)
ES2	1.36 (0.80)	0.019 (0.013)	0.839 (0.558)
ES3	2.15 (1.47)	0.027 (0.021)	1.284 (0.900)
ES group	1.76 (0.39) b <sup>b</sup>	0.023 (0.004) b	1.070 (0.223) b
DS1	9.06 (2.25)	0.172 (0.051)	5.568 (1.503)
DS2	6.95 (3.26)	0.067 (0.026)	4.132 (1.547)
DS3	7.91 (3.17)	0.118 (0.052)	5.306 (2.130)
DS group	7.97 (1.05) a	0.119 (0.053) a	5.002 (0.764) a

RS synthesis rate of <sup>13</sup>C-SOC

<sup>a</sup> ES1, ES2, and ES3 are the three replicates of the eroding site (ES group: abandoned cropland); DS1, DS2, and DS3 are the three replicates of the depositional site (DS group: check dam)

<sup>b</sup> Numbers in brackets are the standard errors of means, and different letters in the same column indicate significant differences at the *P* < 0.05 level based on least significant difference analysis

gullies to check dams resulting in the decreased <sup>137</sup>Cs inventory in depositional sites (check dams). In addition, similar with the <sup>137</sup>Cs distribution, SOC and its labile fractions (DOC and MBC) in the depositional sites were also decreased due to the accumulation of nutrient-poor soil.

High-throughput sequencing of *cbbl* gene revealed that *Proteobacteria* was the dominant phylum of autotrophic bacteria accounting for over 90% OTUs. Confirming what was already reported (Badger and Bek 2008; Esparza et al. 2010; Yuan et al. 2012a), *Alpha*-, *Beta*-, and *Gamma*-*proteobacteria* were the common autotrophic bacterial classes. At the genus level, *Thiobacillus*, *Thioalkalivibrio*, *Alkalispirillum*, *Rhodobacter*, *Nitrosospira*, *Alkalilimnicola*, *Bradyrhizobium*, and *Synechococcus* were the primary autotrophic bacterial taxa. Soil autotrophic microorganisms can be divided into two distinct types: obligate autotrophs and facultative autotrophs (Ge et al. 2012). Obligate autotrophs generally depend on CO<sub>2</sub> as the sole C source for growth, while facultative autotrophs show metabolic flexibility allowing these organisms to grow on organic substrates as alternative C and energy sources (Badger and Bek 2008; Esparza et al. 2010). High organic matter content generally contributes to the rapid growth of facultative autotrophic bacteria in soil (Esparza et al. 2010). Relative to facultative autotrophs, obligate autotrophs are more adapted to the nutrient-poor environments (Badger and Bek 2008; Wu

et al. 2014; Yuan et al. 2012b). Therefore, negative responses of facultative autotrophs (e.g., *Nitrosospira*) to the deposition of nutrient-poor soil were observed. In contrast, the growth of obligate autotrophic bacteria, such as *Thiobacillus* and *Synechococcus*, was improved at depositional sites.

As already reported (Ge et al. 2012; Lynn et al. 2017; Yuan et al. 2015), autotrophic bacterial abundance was positively correlated with SOC and its labile fractions (DOC and MBC). The abundance and diversity of autotrophic bacteria in nutrient-poor depositional sites were significantly lower than those in nutrient-rich eroding sites. This phenomenon may be related to the negative responses of facultative autotrophs to soil deposition. Confirming what was already reported by Lynn et al. (2017) and Yuan et al. (2012a), our results showed that autotrophic bacterial community in soil was dominated by facultative autotrophs (ranged from 59.6 to 82.9%). However, deposition of nutrient-poor soil increased the abundance and diversity of obligate autotrophs, but decreased the abundance of dominant facultative autotrophs. Therefore, the abundance and diversity of total autotrophic bacteria at depositional sites were significantly decreased due to the negative responses of dominant facultative autotrophs to soil deposition. The first hypothesis (H1) that autotrophic bacterial abundance and diversity at the depositional sites would be significantly increased was not supported by our data.

**Table 4** Multiple stepwise regression analysis

Dependent variable	Explaining variables	Coefficients	S.E.	<i>t</i> value	<i>P</i> value	Explained variability (%)
RS ( <sup>13</sup> C-SOC)	Constant	14.761	1.895	7.791	0.000	
	DOC	-35.501	3.869	-9.175	0.000	72.0
	Sand	-0.211	0.054	-3.930	0.002	12.8
	Shannon	-0.960	0.366	-2.621	0.020	4.3
	Adjusted <i>R</i> <sup>2</sup>	0.891				

S.E. standard error; RS synthesis rate of <sup>13</sup>C-SOC; DOC dissolved organic C

After incubation for 80 days, SOC labeled by  $^{13}\text{C}$  was detected in both eroding and depositional sites, suggesting the  $\text{CO}_2$  assimilation by autotrophic bacteria. Microbial C-fixing rate in the study sites ranged from 0.839 to 5.568  $\text{Mg C km}^{-2} \text{ year}^{-1}$  (12 h light exposure). Assuming a total erosion area of  $1.09 \times 10^7 \text{ km}^2$  (Lal 2003), microbial C-fixing potential in eroded landscapes ranged from 0.01 to 0.06  $\text{Pg C year}^{-1}$ , which is lower than the amount of SOC ( $0.37 \text{ Pg C year}^{-1}$ ) released to the atmosphere during erosion (Jacinthe and Lal 2001). Therefore, the effect of microbial  $\text{CO}_2$  assimilation on the C pool recovery of degraded soil is limited. It was reported previously that microbial C-fixing rate was positively correlated with autotrophic bacterial abundance and diversity (Lynn et al. 2017; Tang et al. 2015; Wu et al. 2015). However, an opposite result was observed in our study. Compared with eroding sites with great autotrophic bacterial abundance and diversity, higher microbial C-fixing rate was observed in depositional sites characterized by lower autotrophic bacterial abundance and diversity. This inconsistent result might be related to erosion-induced changes in relative abundances of obligate autotrophic bacteria, most of which obtained C source only by assimilating  $\text{CO}_2$  (Esparza et al. 2010). Relative to facultative autotrophs, obligate autotrophs are more important contributors for microbial  $\text{CO}_2$  assimilation due to their high C-fixing rate (Saini et al. 2011). Therefore, increases in the relative abundances of obligate autotrophic bacteria can contribute to the synthesis of SOC at depositional sites.

Multiple stepwise regression analysis revealed that the DOC content was the main factor explaining the variation in microbial C-fixing rate. Relative to total autotrophic bacterial abundance and diversity, a greater contribution of labile organic fraction to the variation in microbial C-fixing rate was observed. The availability of soil organic matter, to some extent, regulates the proportion of obligate autotrophs and facultative autotrophs in the autotrophic bacterial community. Further, microbial C-fixing rate was affected by the relative proportion between facultative and obligate autotrophs because of their difference in  $\text{CO}_2$  assimilation rate (Badger and Bek 2008; Saini et al. 2011). Through regulating community composition of autotrophic bacteria (i.e., the proportion of obligate autotrophs and facultative autotrophs), erosion-induced changes in soil labile organic matter can influence microbial C-fixing potential. The second hypothesis (H2) that microbial C-fixing rate was mainly controlled by autotrophic bacterial biomass could not be verified. Our study indicated that the abundance and diversity of total autotrophic bacteria might not always reflect their functional activity. By regulating autotrophic bacterial community composition, probably labile organic C was an important factor regulating microbial C-fixing potential.

## Conclusion

Negative responses of total autotrophic bacterial abundance and diversity to deposition of nutrient-poor soil were observed. However, the relative abundances of obligate autotrophic bacteria, such as *Thiobacillus* and *Synechococcus*, were significantly enhanced in depositional sites. The deposition of nutrient-poor soil stimulated the growth of obligate autotrophic bacteria. Microbial C-fixing rate ranged from 0.839 to 5.568  $\text{Mg C km}^{-2} \text{ year}^{-1}$  and was greater in nutrient-poor than in nutrient-rich soils and it was positively correlated with the relative abundances of obligate autotrophic bacteria. But its effect on the C pool recovery of degraded soil was limited. Compared with total autotrophic bacterial abundance and diversity, probably labile organic C was the most important factor regulating microbial C-fixing rate.

**Acknowledgements** We would like to thank Hao Peng of the Hunan University for the soil sample collection.

**Funding information** This work was financially supported by the “Hundred-talent Project” of the Chinese Academy of Sciences and the National Natural Science Foundation of China (41271294).

## References

- Afshar FA, Ayoubi S, Jalalian A (2010) Soil redistribution rate and its relationship with soil organic carbon and total nitrogen using  $^{137}\text{Cs}$  technique in a cultivated complex hillslope in western Iran. *J Environ Radioactiv* 101: 606–614
- Badger MR, Bek EJ (2008) Multiple Rubisco forms in proteobacteria: their functional significance in relation to  $\text{CO}_2$  acquisition by the CBB cycle. *J Exp Bot* 59:1525–1541
- Berhe AA, Harte J, Harden JW, Tom MS (2007) The significance of the erosion-induced terrestrial carbon sink. *Bioscience* 57:337–346
- Cornfield AH (1960) Ammonia released on treating soils with N sodium hydroxide as a possible means of predicting the nitrogen-supplying power of soils. *Nature* 187:260–261
- Doetterl S, Six J, Van Wesemael B, Van Oost K (2012) Carbon cycling in eroding landscapes: geomorphic controls on soil organic C pool composition and C stabilization. *Glob Chang Biol* 18:2218–2232
- Esparza M, Cárdenas JP, Bowien B, Jedlicki E, Holmes DS (2010) Genes and pathways for  $\text{CO}_2$  fixation in the obligate, chemolithoautotrophic acidophile, *Acidithiobacillus ferrooxidans*, carbon fixation in *A. ferrooxidans*. *BMC Microbiol* 10:229
- Gaspar L, Navas A (2013) Vertical and lateral distributions of  $^{137}\text{Cs}$  in cultivated and uncultivated soils on Mediterranean hillslopes. *Geoderma* 207:131–143
- Ge T, Wu X, Chen X, Yuan H, Zou Z, Li B, Zhou P, Liu S, Tong C, Brookes P, Wu J (2013) Microbial phototrophic fixation of atmospheric  $\text{CO}_2$  in China subtropical upland and paddy soils. *Geochim Cosmochim Acta* 113:70–78
- Ge T, Wu X, Liu Q, Zhu Z, Yuan H, Wang W, Whiteley AS, Wu J (2016) Effect of simulated tillage on microbial autotrophic  $\text{CO}_2$  fixation in paddy and upland soils. *Sci Rep* 6:19784
- Ge T, Yuan H, Zhu H, Wu X, Nie SA, Liu C, Tong C, Wu J, Brookes P (2012) Biological carbon assimilation and dynamics in a flooded rice-soil system. *Soil Biol Biochem* 48:39–46

- Jacinthe P, Lal R (2001) A mass balance approach to assess carbon dioxide evolution during erosional events. *Land Degrad Dev* 12:329–339
- Keshri J, Yousuf B, Mishra A, Jha B (2015) The abundance of functional genes, *cbbl*, *nifH*, *amoA* and *apsA*, and bacterial community structure of intertidal soil from Arabian Sea. *Microbiol Res* 175:57–66
- Kjeldahl J (1883) Neue methode zur bestimmung des stickstoffs in organischen körpern. *Fresen J Anal Chem* 22:366–382
- Lal R (2003) Soil erosion and the global carbon budget. *Environ Int* 29:437–450
- Lal R (2005) Soil erosion and carbon dynamics. *Soil Till Res* 81:137–142
- Li ZW, Liu C, Dong YT, Chang XF, Nie XD, Liu L, Xiao HB, Lu Y, Zeng GM (2017) Response of soil organic carbon and nitrogen stocks to soil erosion and land use types in the loess hilly–gully region of China. *Soil Till. Res.* 166:1–9
- Li Z, Xiao H, Tang Z, Huang J, Nie X, Huang B, Ma W, Lu Y, Zeng G (2015) Microbial responses to erosion-induced soil physico-chemical property changes in the hilly red soil region of southern China. *Eur J Soil Biol* 71:37–44
- Liu C, Li Z, Dong Y, Chang X, Nie X, Liu L, Xiao H, Wang D, Peng H (2017) Response of sedimentary organic matter source to rainfall events using stable carbon and nitrogen isotopes in a typical loess hilly-gully catchment of China. *J Hydrol* 552:376–386
- Long XE, Yao H, Wang J, Huang Y, Singh BK, Zhu YG (2015) Community structure and soil pH determine chemoautotrophic carbon dioxide fixation in drained paddy soils. *Environ Sci Technol* 49:7152–7160
- Lynn TM, Ge T, Yuan H, Wei X, Wu X, Xiao K, Kumaresan D, Yu SS, Wu J, Whiteley AS (2017) Soil carbon-fixation rates and associated bacterial diversity and abundance in three natural ecosystems. *Microb Ecol* 73:645–657
- Nie X, Li Z, Huang J, Liu L, Xiao H, Liu C, Zeng G (2018) Thermal stability of organic carbon in soil aggregates as affected by soil erosion and deposition. *Soil Till. Res.* 175:82–90
- Polyakov V, Lal R (2004) Modeling soil organic matter dynamics as affected by soil water erosion. *Environ Int* 30:547–556
- Polyakov V, Lal R (2008) Soil organic matter and CO<sub>2</sub> emission as affected by water erosion on field runoff plots. *Geoderma* 143:216–222
- Saini R, Kapoor R, Kumar R, Siddiqi TO, Kumar A (2011) CO<sub>2</sub> utilizing microbes—a comprehensive review. *Biotechnol Adv* 29:949–960
- Schöler A, Jacquiod S, Vestergaard G, Schulz S, Schloter M (2017) Analysis of soil microbial communities based on amplicon sequencing of marker genes. *Biol. Fert. Soils* 53:485–489
- Selesi D, Pattis I, Schmid M, Kandeler E, Hartmann A (2007) Quantification of bacterial RubisCO genes in soils by *cbbl* targeted real-time PCR. *J Microbiol Meth* 69:497–503
- Stallard RF (1998) Terrestrial sedimentation and the carbon cycle: coupling weathering and erosion to carbon burial. *Global Biogeochem Cy* 12:231–257
- Tang ZX, Fan FL, Wan YF, Wei W, Lai LM (2015) Abundance and diversity of RuBisCO genes responsible for CO<sub>2</sub> fixation in arid soils of northwest China. *Pedosphere* 25:150–159
- Vestergaard G, Schulz S, Schöler A, Schloter M (2017) Making big data smart—how to use metagenomics to understand soil quality. *Biol Fert Soils* 53:479–484
- Videmsek U, Hagn A, Suhadolc M, Radl V, Knicker H, Schloter M, Vodnik D (2009) Abundance and diversity of CO<sub>2</sub>-fixing bacteria in grassland soils close to natural carbon dioxide springs. *Microbiol Ecol* 58:1–9
- Walkley A, Black IA (1934) An examination of the Degtjareff method for determining soil organic matter, and a proposed modification of the chromic acid titration method. *Soil Sci* 37:29–38
- Wang Y, Fang N, Zhang F, Wang L, Wu G, Yang M (2017) Effects of erosion on the microaggregate organic carbon dynamics in a small catchment of the Loess Plateau, China. *Soil Till Res* 174:205–213
- Wu X, Ge T, Wang W, Yuan H, Wegner CE, Zhu Z, Whiteley AS, Wu J (2015) Cropping systems modulate the rate and magnitude of soil microbial autotrophic CO<sub>2</sub> fixation in soil. *Front Microbiol* 6:379
- Wu X, Ge T, Yuan H, Li B, Zhu H, Zhou P, Sui F, O'Donnell AG, Wu J (2014) Changes in bacterial CO<sub>2</sub> fixation with depth in agricultural soils. *Appl Microbiol Biotechnol* 98:2309–2319
- Xiao H, Li Z, Chang X, Huang J, Nie X, Liu C, Liu L, Wang D, Dong Y, Jiang J (2017a) Soil erosion-related dynamics of soil bacterial communities and microbial respiration. *Appl Soil Ecol* 119:205–213
- Xiao H, Li Z, Dong Y, Chang X, Deng L, Huang J, Nie X, Liu C, Liu L, Wang D, Liu Q, Zhang Y (2017b) Changes in microbial communities and respiration following the revegetation of eroded soil. *Agric Ecosyst Environ* 246:30–37
- Xu XZ, Zhang HW, Zhang OY (2004) Development of check-dam systems in gullies on the Loess Plateau, China. *Environ Sci Pol* 7:79–86
- Yuan H, Ge T, Chen C, O'Donnell AG, Wu J (2012a) Significant role for microbial autotrophy in the sequestration of soil carbon. *Appl Environ Micro* 78:2328–2336
- Yuan H, Ge T, Chen X, Liu S, Zhu Z, Wu X, Wei W, Whiteley AS, Wu J (2015) Abundance and diversity of CO<sub>2</sub>-assimilating bacteria and algae within red agricultural soils are modulated by changing management practice. *Microb Ecol* 70:971–980
- Yuan H, Ge T, Wu X, Liu S, Tong C, Qin H, Wu M, Wei W, Wu J (2012b) Long-term field fertilization alters the diversity of autotrophic bacteria based on the ribulose-1,5-biphosphate carboxylase/oxygenase (RubisCO) large-subunit genes in paddy soil. *Appl Microbiol Biotechnol* 95:1061–1071
- Yuan H, Ge T, Zou S, Wu X, Liu S, Zhou P, Chen X, Brookes P, Wu J (2012c) Effect of land use on the abundance and diversity of autotrophic bacteria as measured by ribulose-1,5-biphosphate carboxylase/oxygenase (RubisCO) large subunit gene abundance in soils. *Biol Fert Soils* 49:609–616
- Yuan H, Zhu Z, Liu S, Ge T, Jing H, Li B, Liu Q, Lynn TM, Wu J, Kuzyakov Y (2016) Microbial utilization of rice root exudates: <sup>13</sup>C labeling and PLFA composition. *Biol Fert Soils* 52:615–627
- Zhou SM, Lei TW, Warrington DN, Lei QX, Zhang ML (2012) Does watershed size affect simple mathematical relationships between flow velocity and discharge rate at watershed outlets on the Loess Plateau of China. *J Hydrol* 444:1–9